Supplementary Material for "Mottness at finite doping and charge-instabilities in cuprates"

OPTICAL PROPERTIES OF $Bi_2Sr_{2-x}La_xCuO_{6+\delta}$ AT EQUILIBRIUM

In Figure S1 we report the light penetration depth in La-Bi2201, as a function of the photon energy at different doping concentrations. The penetration depth (d_{pen}) has been obtained from the La-Bi2212 optical conductivity that has been measured elsewhere [6]. Since the density of the CT excitations induced by the pump pulse depends on the energy density delivered by the pump pulse, the knowledge of d_{pen} is necessary to maintain a constant excitation density when the doping is changed. As shown in Figure S1, at the pump photon energy of 1.4 eV d_{pen} decreases as the doping is increased. This is the consequence of the progressive increase of the charge carrier density which results in a larger Drude contribution to the absorption process. The incident fluence has been tuned in order to maintain a constant excitation density of 7 J/cm^3 for all the time-resolved measurements at different doping concentrations.

ULTRAFAST REFLECTIVITY VARIATION IN THE UV-VIS SPECTRAL RANGE

In order to rule out the possibility that, in optimally and over-doped La-Bi2201 samples, the absence of the CT redhsift is related to a large increase of the Δ_{CT} energy, which would push the observed phenomenon out of the explored energy window, we extended the time-resolved measurements up to an energy of 3 eV. In Figure S2 we report the $\delta R(\omega,t)/R$ matrix measured on the overdoped La-Bi2201 sample (p=0.2). The absence of any negative component in the signal, allows us to conclude that no CT redshift is observed in the energy range that extends far above the Δ_{CT} energy estimated by equilibrium optical spectroscopy. The same experiment has been repeated at different pump photon energies ($\hbar\omega$ = 2.06 eV and $\hbar\omega$ = 1.77 eV). The measured dynamics did not evidence any significant change, in agreement with the results reported in the main text.

ULTRAFAST OPTICAL SPECTROSCOPY AT DIFFERENT TEMPERATURES

The transition of the CT dynamics observed in the La-Bi2201 samples at room temperature and at p=p_{cr} is uncorrelated with the onset of the pseudogap at low temperatures. This can be easily inferred by single-color reflectivity measurements on the p=0.16 La-Bi2201 sample at different temperatures, as shown in Figure S3. The data have been collected starting from a cavity-dumped Ti:Sapphire oscillator. The photon energies are set to 3.14 and 1.5 eV for the pump and the probe, respectively. The fluence is of the order of 10 μJ/cm^2. Panel a) shows the time traces at different temperatures. The onset of a negative component, typical of the pseudogap phase [1] is observed below a temperature T^* $\simeq$100 K. A double exponential function $\delta R(\tau)/R = A_1 e^{\frac{-t}{\tau_1}} + A_2 e^{\frac{-t}{\tau_2}}$ is fit to the measured time traces. While the first exponential is positive and accounts for the typical electron-phonon dynamics of the normal state [3], the amplitude of the second decay A_2 is negative and accounts for the dynamics in the pseudogap region [1]. In Figure S3 we report the absolute value of the ratio between the negative and the positive contributions (A_2/A_1) as a function of the temperature. The A_2 component vanishes at T^* $\simeq$100 K demonstrating that the pseudogap onset is at temperatures significantly smaller that the temperature at which the $p = p_{cr}$ discontinuity is observed.

The Mottness in the $p < p_{cr}$ region of the phase diagram involves energy scales corresponding to Δ_{CT}=2 eV. The dynamics at such a high energy scale is expected to be completely temperature independent, being the thermal fluctuations confined to k_BT. In order to support this assumption, we performed frequency- and time-resolved measurements at different temperatures. In particular, we focused on the optimally doped sample that is the closest to the p_{cr} turning point. In order to avoid artifacts related to the impulsive heating of the sample when the temperature is decreased we performed time-resolved measurements in the low-fluence regime ($\simeq$10 μJ/cm^2). The relative reflectivity variation, $\delta R(\omega,t)/R$, has been measured exploiting the supercontinuum light produced by a photonic fiber seeded by a cavity-dumped Ti:sapphire oscillator. The details of the experimental setup can be found in Refs. 5 and **?** The frequency- and time-resolved reflectivity maps are reported in Figure S3c. In order to avoid effects related to the increased average heating at low temperature, the repetition rate (RR) of the experiment has been decreased as to maintain the ratio RR/$C_{tot}(T)$ constant, $C_{tot}(T)$ being the total heat capacity. The data reported in the figure demonstrate that the $\delta R(\omega,t)/R$ signal at the Δ_{CT} energy scale is temperature independent and that the transition

observed at p_{cr} does not represent the room-temperature intersection with an additional $\tilde{T}(p)$ line that decreases as the doping increases.

RESONANT SOFT X-RAY SCATTERING (RXS) ON $Bi_2Sr_{2-x}La_xCuO_{6+\delta}$

In Fig. S5 we show resonant soft X-ray scattering (RXS) measurements on $Bi_2Sr_{2-x}La_xCuO_{6+\delta}$ at three different level of doping. These data are readapted from [2]. The resonance in the RXS signal at T=10 K at momentum $\mathbf{Q}_{\parallel} = 0.27$ underlines the presence of a spontaneous breaking of the translational symmetry of the charge distribution within the CuO_2 planes. The amplitude of the charge density modulation ($\langle \delta_{CDW} \rangle$) shown in Fig. 3 of the main text for different doping is evaluated integrating the RXS signal along the whole probed momenta at T=10 K and normalizing it on the integrated intensity at T=300 K.

[1] F. Cilento, S. Dal Conte, G. Coslovich, S. Peli, N. Nembrini, S. Mor, F. Banfi, G. Ferrini, H. Eisaki, M. K. Chan, C. J. Dorow, M. J. Veit, M. Greven, D. van der Marel, R. Comin, A. Damascelli, L. Rettig, U. Bovensiepen, M. Capone, C. Giannetti, and F. Parmigiani. Photo-enhanced antinodal conductivity in the pseudogap state of high-tc cuprates. *Nat Commun*, 5, 07 2014. URL `http://dx.doi.org/10.1038/ncomms5353`.

[2] R. Comin, A. Frano, M. M. Yee, Y. Yoshida, H. Eisaki, E. Schierle, E. Weschke, R. Sutarto, F. He, A. Soumyanarayanan, Yang He, M. Le Tacon, I. S. Elfimov, Jennifer E. Hoffman, G. A. Sawatzky, B. Keimer, and A. Damascelli. Charge order driven by fermi-arc instability in $Bi_2Sr_{2-x}La_xCuO_{6+\delta}$. *Science*, 343(6169):390–392, 2014. doi: 10.1126/science.1242996.

[3] S. Dal Conte, C. Giannetti, G. Coslovich, F. Cilento, D. Bossini, T. Abebaw, F. Banfi, G. Ferrini, H. Eisaki, M. Greven, A. Damascelli, D. van der Marel, and F. Parmigiani. Disentangling the electronic and phononic glue in a high-tc superconductor. *Science*, 335(6076):1600–1603, 03 2012. URL `http://www.sciencemag.org/content/335/6076/1600.abstract`.

[4] S. Dal Conte, L. Vidmar, D. Golez, M. Mierzejewski, G. Soavi, S. Peli, F. Banfi, G. Ferrini, R. Comin, B. M. Ludbrook, L. Chauviere, N. D. Zhigadlo, H. Eisaki, M. Greven, S. Lupi, A. Damascelli, D. Brida, M. Capone, J. Bonca, G. Cerullo, and C. Giannetti. Snapshots of the retarded interaction of charge carriers with ultrafast fluctuations in cuprates. *Nat Phys*, 11(5):421–426, 05 2015. URL `http://dx.doi.org/10.1038/nphys3265`.

[5] Claudio Giannetti, Federico Cilento, Stefano Dal Conte, Giacomo Coslovich, Gabriele Ferrini, Hajo Molegraaf, Markus Raichle, Ruixing Liang, Hiroshi Eisaki, Martin Greven, Andrea Damascelli, Dirk van der Marel, and Fulvio Parmigiani. Revealing the high-energy electronic excitations underlying the onset of high-temperature superconductivity in cuprates. *Nat Commun*, 2:353, 06 2011. URL `http://dx.doi.org/10.1038/ncomms1354`.

[6] S. Lupi, D. Nicoletti, O. Limaj, L. Baldassarre, M. Ortolani, S. Ono, Yoichi Ando, and P. Calvani. Far-infrared absorption and the metal-to-insulator transition in hole-doped cuprates. *Phys. Rev. Lett.*, 102:206409, May 2009. doi: 10.1103/PhysRevLett.102.206409. URL `http://link.aps.org/doi/10.1103/PhysRevLett.102.206409`.

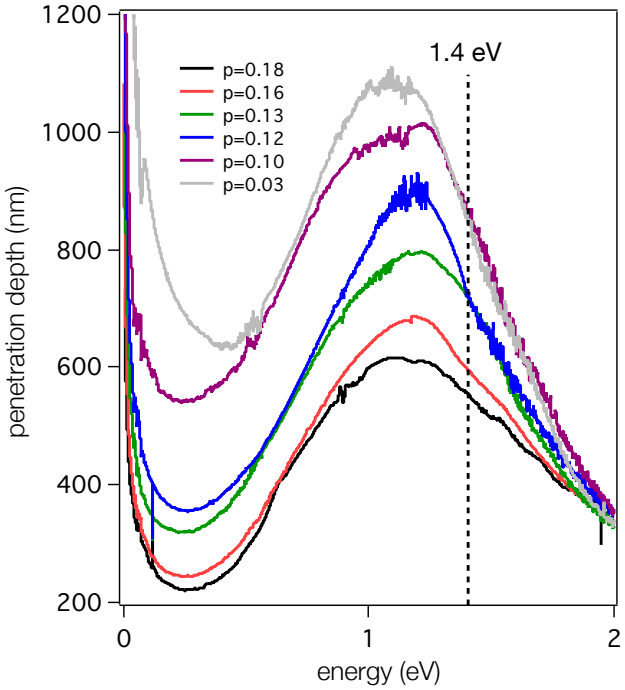

Figure S 1: Penetration depth in $Bi_2Sr_{2-x}La_xCuO_{6+\delta}$, as a function of the photon energy and for different doping concentrations, $0.03 < p < 0.18$. The photon energy of the pump pulse (1.4 eV) is indicated by a black line.

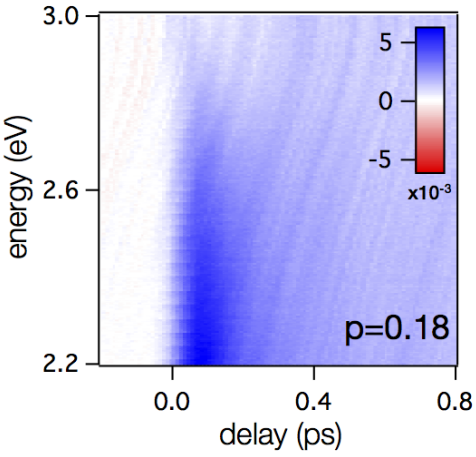

Figure S 2: Ultrafast reflectivity variation $(\delta R(\omega, t)/R)$ measured by optical spectroscopy on the p=0.2 La-Bi2201 sample. The pump photon energy was set at 2.06 eV. The colour scale is reported in the inset.

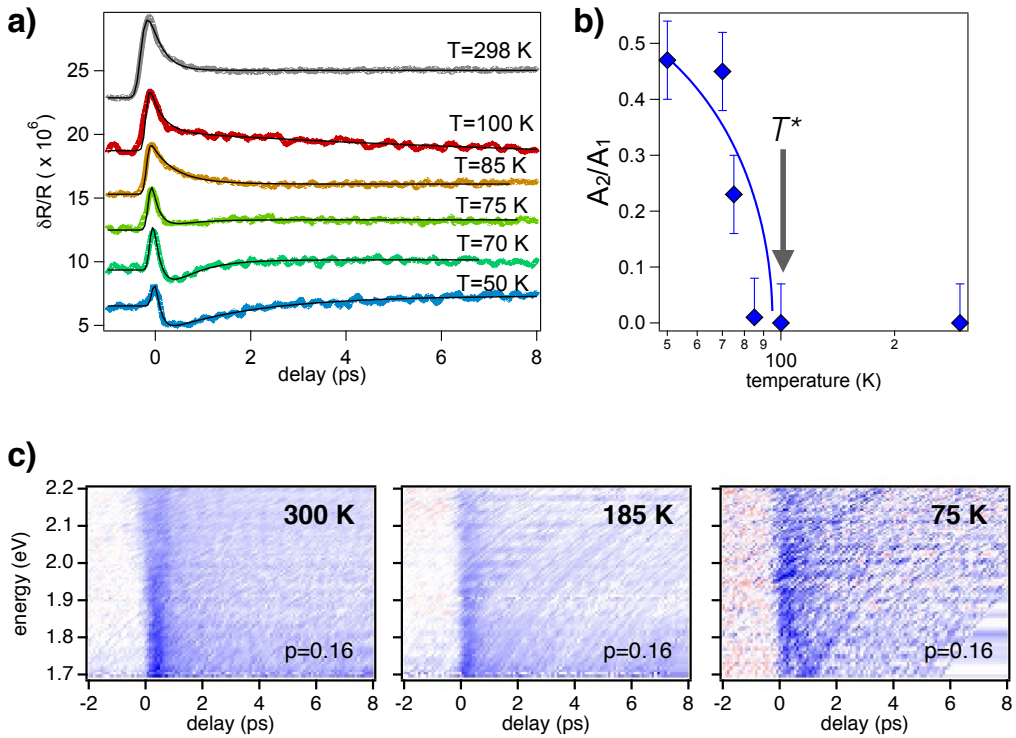

Figure S 3: a) Single-color ultrafast reflectivity variation ($\delta R(t)/R$) maesured at different temperatures on the p=0.16 La-Bi2201 sample. The solid black lines represent the bi-exponential fit to the data. b) The ratio (A_2/A_1) of the amplitude of the two exponential functions is reported as a function of the temperature. The solid line is a guide to the eye. c) Ultrafast dynamics at the Δ_{CT} energy scale at different temperatures. The color scale is the same than that used in Figure S2

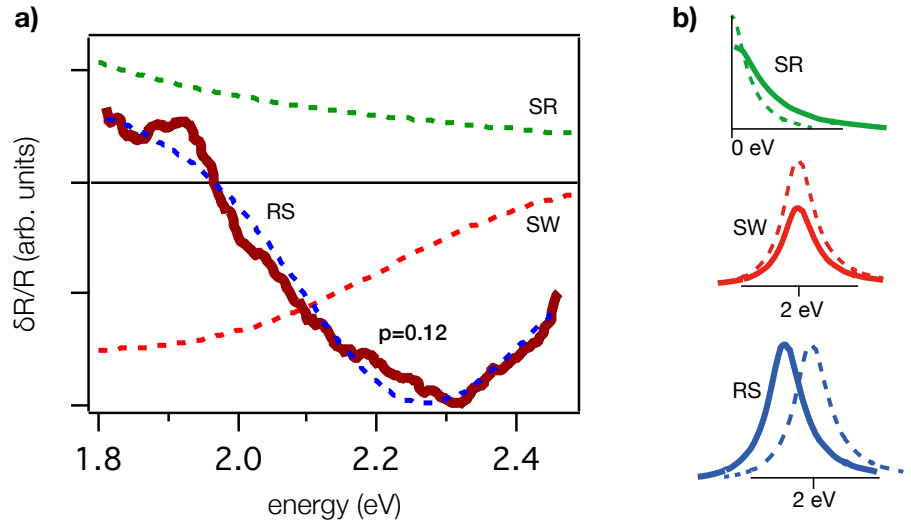

Figure S 4: a) $\delta R(\omega,\tau)/R$ (purple solid line) measured on the p=0.12 La-Bi2201 sample at a delay τ=50 fs. The dashed lines are the reflectivity variations calculated by modifying different parameters in the equilibrium dielectric function. In particular, we considered the increase of the total scattering rate in the Drude part of the optical conductivity (dashed green line, SR), the redshift of Δ_{CT} (dashed blue line, RS) and the change of the CT spectral weight (dashed red line, SW). b) A pictorial view of the modification of the optical conductivity for the three cases is reported.

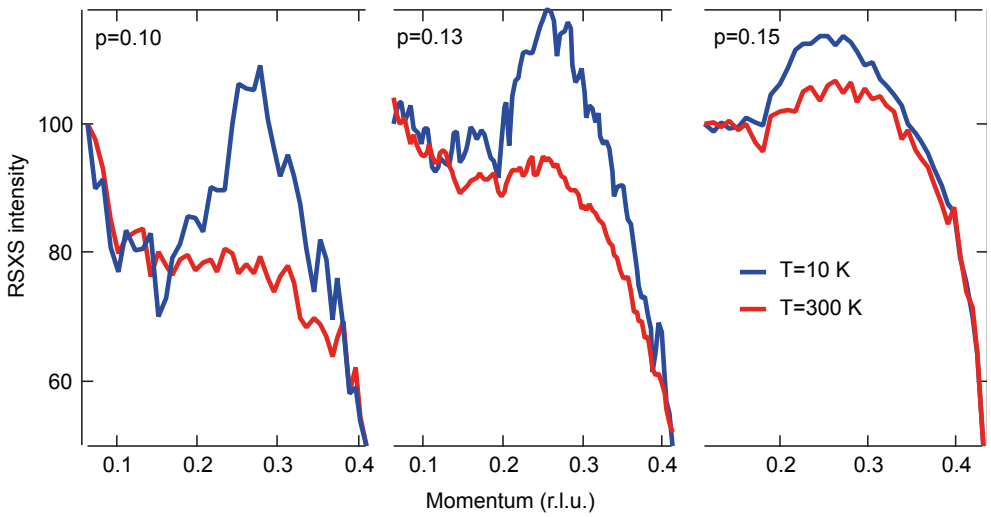

Figure S 5: Low- and high-temperature scattering scans for the doping levels investigated with RXS: $p = 0.10$, $p = 0.13$, $p = 0.15$ [2].